J|A|C|S
ARTICLES
Published on Web 01/03/2007

Photon-Induced Selective Interaction between Small-Diameter Metallic Carbon Nanotubes and Triton X-100

Zhi-Bin Zhang† and Shi-Li Zhang*,†,‡

Contribution from the School of Information and Communication Technology, Royal Institute of Technology, Electrum 229, SE-164 40 Kista, Sweden, and School of Microelectronics, Fudan University, Shanghai 200433, China

Received September 5, 2006; E-mail: shili@kth.se

Abstract: We report a highly selective chemical interaction between single-walled carbon nanotubes and Triton X-100 according to nanotubes' electronic structure and diameter. The interaction is induced by laser irradiation at power densities down to 10^{-2} μW/μm^2 but with photon energies matching those for electronic transition in nanotubes. Our experimental results point to a photon-induced chemical interaction of Triton X-100 with metallic nanotubes below 1.1 nm in diameter and indicate the selectivity being dictated by Fermi electrons and enhanced by curvature-induced strain.

Introduction

Single-walled carbon nanotubes (SWNTs) are of great potential for a vast variety of applications due to their unique structural, mechanical, thermal, electrical, and optical properties.[1] However, all known synthetic techniques to date lead to the growth of a mixture of SWNTs in both metallic and semiconducting types with various chiralities and diameters. Postsynthesis treatments aiming at separation of SWNTs by diameter and type are hence crucial for fundamental research as well as practical applications. Significant progress has been made toward a selective control of SWNTs according to their diameter or type by using chemical, physical, or biological approaches. As an example, sidewall chemical functionalization of SWNTs by ozonolysis has been shown to have a diameter selectivity.[2] Most of the studied methods for SWNT separation by type rely on selective interactions of metallic (m-) and semiconducting (s-) SWNTs with chemical/biomolecular species including octadecylamine (ODA),[3] bromine,[4] nitronium ions,[5] and DNA.[6] The difference in dielectrophoretic response between m-SWNTs and s-SWNTs to a nonuniform AC electric field has been used for separation of m-SWNTs from s-SWNTs.[7] A further method for selective removal of one specific charility of SWNTs relies on photon-assisted oxidation with laser irradiation at sufficient power densities.[8,9] For s-SWNTs in solution phase, the redox chemistry has been found with a tendency of chirality selectivity.[10,11] Despite the significant progress so far, none of the selection methods for a specific kind of SWNT are viable for ultimate material homogeneity. Further investigation and development is desirable.

In this Article, we report a simple method for chemical functionalization of SWNTs by Triton X-100 with a high selectivity by type and diameter. Various surfactants have been widely employed to stabilize individual SWNTs in solution for subsequent studies of their electronic transitions using Raman spectroscopy, photoluminescence, and optical adsorption, because surfactants interact with nanotubes through physisorption without perturbing the electronic structure of SWNTs.[12] These surfactants include Triton X-100 ($C_8H_{17}C_6H_4(OCH_2CH_2)_nOH$) that is a non-ionic surfactant with a hydrophilic polyethylene oxide (PEO) group at one end and a hydrocarbon hydrophobic group with a phenyl ring at the other end (Figure 1). On average, Triton X-100 comprises 9.5 ethylene oxide units (i.e., $n = 9.5$). It was used here for solubilizing SWNTs in water owing to the steric repulsion of the hydrophilic oxide group. In an effort to characterize SWNTs dispersed in condensed aqueous Triton X-100 solution by means of Raman spectroscopy, we discovered a strong selectivity in bleaching the Raman signals originating from m-SWNTs less than 1.1 nm in diameter. No change was found to the Raman signals from s-SWNTs. The Raman signals from m-SWNTs greater than 1.1 nm in diameter also remained intact. These phenomena persisted at low laser power densities

† Royal Institute of Technology.
‡ Fudan University.

(1) Dresselhaus, M. S.; Dresselhaus, G.; Avouris, Ph. *Carbon Nanotubes: Synthesis, Structure, Properties, and Applications*; Springer-Verlag: Berlin, 2001.
(2) Banerjee, S.; Wong, S. S. *Nano Lett.* **2004**, *4*, 1445.
(3) Chattopadhyay, D.; Galeska, I.; Papadimitrakopoulos, F. *J. Am. Chem. Soc.* **2003**, *125*, 3370.
(4) Chen, Z.; Du. X.; Du, M. H.; Rancken, C. D.; Cheng, H. P.; Rinzler, A. G. *Nano Lett.* **2004**, *3*, 1245.
(5) An, K. H.; Park, J. S.; Yang, C. M.; Jeong, S. Y.; Lim, S. C.; Kang, C.; Son, J. H.; Jeong, M. S.; Lee, Y. H. *J. Am. Chem. Soc.* **2005**, *127*, 5196.
(6) Zheng. M.; Jagota, A.; Semke, E. D.; Diner, B. A.; Mclean, R. S. *Nature Mater.* **2003**, *2*, 338.
(7) Krupke, R.; Hennrich, F.; Löhneysen, H.; Kappes, M. *Science* **2003**, *301*, 344.
(8) Yudasaka, M.; Zhang, M.; Iijima, S. *Chem. Phys. Lett.* **2003**, *374*, 132.
(9) Maehashi, K.; Yasuhide, O.; Inoue, K.; Matsumoto, K. *Appl. Phys. Lett.* **2004**, *85*, 858.
(10) Zheng. M.; Diner, B. A. *J. Am. Chem. Soc.* **2004**, *126*, 15490.
(11) O'Connell, M. J.; Eibergen, E. E.; Doorn, S. K. *Nature Mater.* **2005**, *4*, 412.
(12) O'Connell, M. J.; Bachilo, S. M.; Huffman, C. B.; Moore, V. C.; Strano, M. S.; Haroz, E. H.; Rialon, K. L.; Boul, P. J.; Noon, W. H.; Kittrell, C.; Ma, J.; Hauge, R. H.; Weisman, R. B.; Smalley, R. E. *Science* **2002**, *297*, 593.

10.1021/ja066419s CCC: $37.00

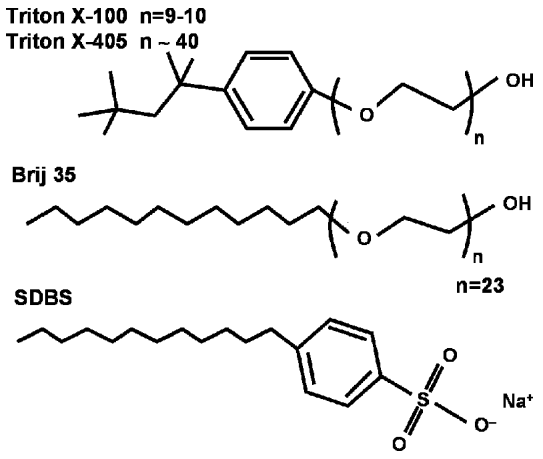

Figure 1. Chemical structures of the surfactants used in this work: Triton X-100 and X-405 (upper), Brij 35 (middle), and sodium dodecylbenzene sulfonate, SDBS (lower).

down to 10^{-2} μW/μm^2. These findings can be of practical implications in fostering a viable SWNT separation scheme, which is important for nanotube-based nanoelectronics and sensors. In what follows, our focus is placed on scrutinizing the details pertaining to the interaction of SWNTs with Triton X-100.

Experimental Section

Raw HiPCO SWNT soot with an average tube diameter of 1.1 nm and weighing 1.4 mg in total was suspended in a 10-mL aqueous Triton X-100 solution. The solution comprised 1 wt % Triton X-100 in deionized (DI) water. The suspension first underwent a bath sonication for 12 h. The resultant dispersion was subsequently treated by cup-horn sonicator at 40 W for 30 min during which the polypropylene test tube containing the dispersion was kept in ice for cooling. The dispersion was then centrifuged at 16000*g* for 16 h. The upper 50% in volume of the supernatant was decanted and stored in a new polypropylene test tube for further use, whereas the remaining 50% supernatant was discarded. The sediment that mainly contained big SWNT bundles was also kept for investigation.

Individual drops of the supernatant and sediment, 10 μL each, were placed onto an oxidized Si substrate with the assistance of a pipet. They were kept in air at room-temperature typically for 1 h until the dispersion became dry. Each drop occupied a surface area around 1 cm^2 on the SiO_2 surface (i.e., the surface of the oxidized Si). In this way, a film of HiPCO SWNTs dispersed in condensed aqueous Triton X-100 solution was formed on the SiO_2 surface. For clarity, the samples are denoted SUP for the supernatant on SiO_2 and SED for the sediment on SiO_2. A reference, denoted PRI, was also prepared by depositing the HiPCO SWNTs dispersed in ethanol on the oxidized Si. For a valid comparison, no analysis was performed on the reference until complete evaporation of the ethanol. A further, yet rather preliminary, comparison was made between Triton X-100 and two other non-ionic surfactants, Triton X-405 ($C_8H_{17}C_6H_4(OCH_2CH_2)_nOH$, $n \sim 40$) and Brij 35 ($C_{12}H_{25}(OCH_2CH_2)_nOH$, $n \sim 23$) whose structures are also depicted in Figure 1. A nominally identical surfactant concentration for each nanotube suspension was used. The sample preparation procedure was simplified by omitting the bath sonication and centrifuge steps. The present study puts a focus on Triton X-100 since its use gave rise to more significant and rapid changes of the Raman signals than what Triton X-405 and Brij 35 did (see Supporting Information).

Resonant Raman spectroscopy (RRS) was employed as our primary tool for laser irradiation as well as for characterization of the samples at two wavelengths 514.5 nm (Ar^+ ion laser) and 632.8 nm (He−Ne laser). The power for the 514.5-nm laser was adjusted from 1 mW to 100 mW while that for the 632.8-nm laser was kept at 20 mW. The

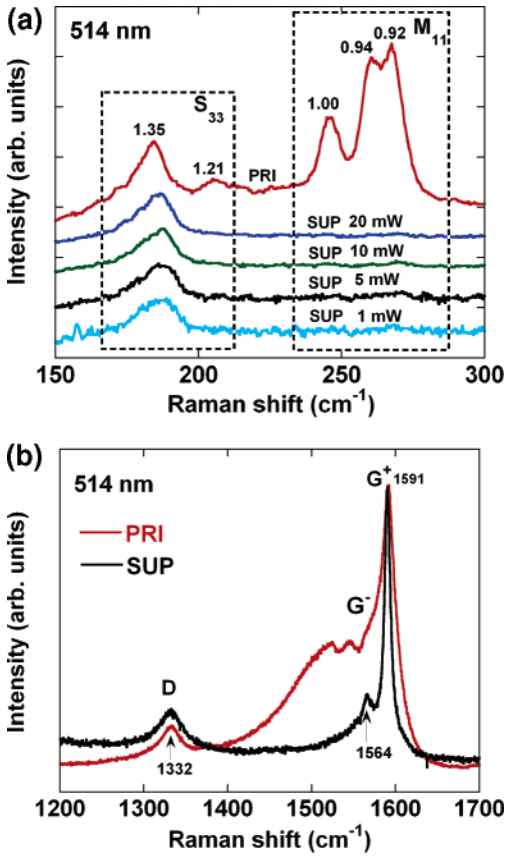

Figure 2. Resonant Raman spectra at 514.5 nm wavelength in (a) the RBM section for sample PRI acquired at 20 mW and sample SUP acquired at different power levels, and (b) the G and D bands for samples PRI and SUP both acquired at 20 mW, with a preirradiation for 4 min at the same power as that for data acquisition.

objective of the optical system was set to 10×, which yielded a spot size on the SiO_2 surface of around 130 μm in diameter in order to obtain Raman signals from large amounts of SWNTs within a single light spot. As RRS plays a central role in the present work, a brief account of how it works is necessary prior to presentation and discussion of the experimental results. When the energy of the incident laser matches the allowed electronic transitions between van Hove singularities of a particular nanotube, Raman signals of the nanotube are resonantly enhanced. Thus, laser excitation at different wavelengths brings nanotubes of different diameters into resonance, which is described by Kataura plot.[13] A Raman spectrum of SWNTs has three important sections: (a) the radial breathing mode (RBM) in the frequency interval 150−300 cm^{-1} in which the peaks are dependent on the nanotube diameter; (b) the tangential mode (G band) in 1400−1700 cm^{-1}; (c) the disorder-induced mode (D band) in 1280−1320 cm^{-1}.

Results and Discussion

(a) Excitation at 514.5 nm. The RBM section of the Raman spectra excited at 514.5 nm is depicted in Figure 2a, whereas the D and G bands are shown in Figure 2b for samples PRI and SUP. For each Raman spectrum, the laser was kept irradiating on one spot of a sample for 4 min followed by immediate data acquisition for 30 s at the same power. The same process was repeated for acquiring another spectrum at a different laser power, yet always on a fresh spot of the sample. In Figure 2a, the spectra are separated and displaced vertically

(13) Kataura, H.; Kumazawa, Y.; Maniwa, Y.; Uemezu, I.; Suzuki, S.; Ohtsuka, Y.; Achiba, Y. *Synth. Met.* **1999**, *103*, 2555.

for clarity after normalization to the integrated peak intensity of the first peak to the left marked 1.35 atop. At 514.5 nm, the excitation is resonant with the v1 → c1 transition (M_{11}) in m-SWNTs with a diameter below 1.1 nm. Simultaneously, it is resonant with the v3 → c3 transition (S_{33}) in s-SWNTs with a diameter above 1.1 nm. As shown on the spectrum for sample **PRI**, the RBM peaks at 246, 260, and 268 cm^{-1} are categorized to the M_{11} band where those at 184 and 205 cm^{-1} to the S_{33} band. The diameter values in nm marked on top of the RBM peaks were obtained according to the following empirically relation for HiPCO SWNTs:[14]

$$\omega_{\mathrm{RBM}} = \frac{223.5}{d_t} + 12.5 \qquad (1)$$

with ω_{RBM} as the RBM frequency and d_t the nanotube diameter.

While the S_{33} peak marked 1.35 only differs slightly in frequency between samples PRI and SUP, a striking difference is observed with respect to the M_{11} band in Figure 2a; the M_{11} peaks for sample PRI are the most intense, but such peaks are practically invisible for sample SUP. Furthermore, the intense M_{11} peaks remained unchanged when the same spot was repeatedly irradiated at 20 mW for sample PRI. But these peaks never showed up for sample SUP by reducing the irradiation power successively from 20 to 1 mW (i.e., 0.075 $\mu W/\mu m^2$). The lowest power achievable with our Raman spectroscopy setup was 1 mW . Although the overall signal intensity was decreased with decreasing power under otherwise the same experimental conditions, the characteristic outcome of the Raman spectra remained the same as shown in Figure 2a, indicating that the physics behind the observed phenomena is independent of the laser power intensity. The slight upshift by 2 cm^{-1} for the S_{33} peak marked 1.35 for sample SUP as compared to sample PRI, i.e., 186 versus 184 cm^{-1}, which has also been reported for SWNTs dispersed in aqueous sodium dodecyl sulfate (SDS) solution in the literature,[15] as well as the absence of the S_{33} peak marked 1.21 for sample SUP, is probably caused by physisorption of Triton X-100 on the sidewall of s-SWNTs.

To confirm the effect of Triton X-100, several experiments were performed and the Raman investigation was carried out at 514.5 nm and 20 mW. First, by washing sample SUP in DI water for 24 h *prior to* Raman investigation, the M_{11} peaks did appear with an appreciable intensity with reference to the S_{33} peak marked 1.35. Only a slight decrease of the intensity of the M_{11} peaks was found after laser irradiation for 6 min. This small decrease in M_{11} peak intensities could be attributed to the presence of Triton X-100 residuals on the sidewalls of SWNTs after the intensive wash. Second, by reversing the procedure to bake in air at 160 °C for 3 h or to wash in DI water of the sample *after* having performed the laser irradiation at 20 mW on the same spot in sample SUP, no M_{11} peak could be found. Third, all Raman peaks including those in the M_{11} and S_{33} bands appeared and remained unaltered during repeated Raman investigations for samples with SWNTs dispersed in aqueous Triton X-100 without drying. Apparently, the concentration of Triton X-100 is a crucial factor in affecting the subsequent Raman analysis results. Fourth, samples similar to SUP were made but instead with the use of sodium dodecylbenzene sulfonate (SDBS, $C_{12}H_{25}C_6H_4SO_3Na$), see Figure 1, as the surfactant. The M_{11} peaks appeared with an appreciable intensity with respect to that of the S_{33} peak, and no decay of them was found during similar repeated laser irradiations at 20 mW, except for a minor peak shift and intensity redistribution compared to sample PRI (see Supporting Information).

The formation of a covalent linkage of chemical species to the sidewall of nanotubes has been shown[2,16−18] to give rise to a substantial decay of spectral peaks as a result of localization of electrons and destruction of the electronic band structure of functionalized nanotubes. Consequently, no resonance with the incident laser occurs. Redox reaction occurring on nanotubes with active agents has also been demonstrated to lead to spectral bleaching mainly resulting from electron-transfer kinetics.[10,11] Physisorption, e.g., via van der Waals force, of surfactants or polymers on nanotubes may cause a spectral shift and intensity redistribution, but it does not lead to spectral decay since the electronic structure of a nanotube is undisturbed.[19] Therefore, the disappearance or absence of the M_{11} peaks in Figure 2a for sample SUP suggests a chemical reaction occurring on the sidewall of m-SWNTs below 1.1 nm in diameter in our sample, which is clearly induced and facilitated by laser irradiation at 514.5 nm. This reaction most likely results in chemical interaction between Triton X-100 and m-SWNTs. Such a chemical interaction is obviously absent between Triton X-100 and s-SWNTs above 1.1 nm in diameter. On the other hand, it is unlikely that the absence of the M_{11} peaks in sample SUP is caused by destruction of m-SWNTs and formation of amorphous carbon, as has been reported to occur in the presence of nitronium ions.[5] Although oxygen could be present, as it could be dissolved in the aqueous Triton X-100 solution or come from the experimental environment (air), the chemistry used in the present work was simple and there was no other chemical reagent than Triton X-100 in DI water. Furthermore, the power density used for laser irradiation was kept low.

The important role of Triton X-100 in selectively bleaching the M_{11} peaks excited at 514.5 nm is now established. But Triton X-100 alone is unlikely to accomplish the bleach observed. Laser irradiation with appropriate photon energies is another critical factor leading to the selective bleach, which will receive further discussions later. To conclude, the different behavior with the M_{11} peaks excited at 514.5 nm between samples PRI and SUP indicates a strong selectivity by the electronic structure of SWNTs, i.e., m-SWNTs versus s-SWNTs, in terms of the interaction with Triton X-100 under laser irradiation at 514.5 nm.

The strong selectivity caused by Triton X-100 in bleaching Raman signals by the electronic type of SWNTs is supported by the different behaviors with the G band in Figure 2b. For sample PRI, the G band has a typical Breit−Wigner−Fano (BWF) line shape with a broad G^- component around 1564

(14) Bachilo, S. M.; Strano, M. S.; Kittrell, C.; Hauge, R. H.; Smalley, R. E.; Weisman, R. B. *Science* **2002**, *298*, 2361.
(15) Fantini, C.; Jorio, A.; Souza, M.; Dresselhaus, M. S.; Pimenta, M. A. *Phys. Rev. Lett.* **2004**, *93*, 147406.
(16) Strano, M. S.; Dyke, C. A.; Usrey, M. L.; Barone, P. W.; Allen, M. J.; Shan, H.; Kittrell, C.; Hauge, R. H.; Tour, J. M.; Smalley, R. E. *Science* **2003**, *301*, 1519.
(17) Banerjee, S.; Wong, S. S. *J. Phys. Chem. B* **2002**, *106*, 12144.
(18) Marcoux, P. R.; Schreiber, J.; Batail, P.; Lefrant, S.; Renouard, J.; Jacob, G.; Albertini, D.; Mevellec, J. T. *Phys. Chem. Chem. Phys.* **2002**, *4*, 2278.
(19) Moor, V. C.; Strano, M. S.; Haroz, E. H.; Hauge, R. H.; Smalley, R. E. *Nano Lett.* **2003**, *3*, 1379.

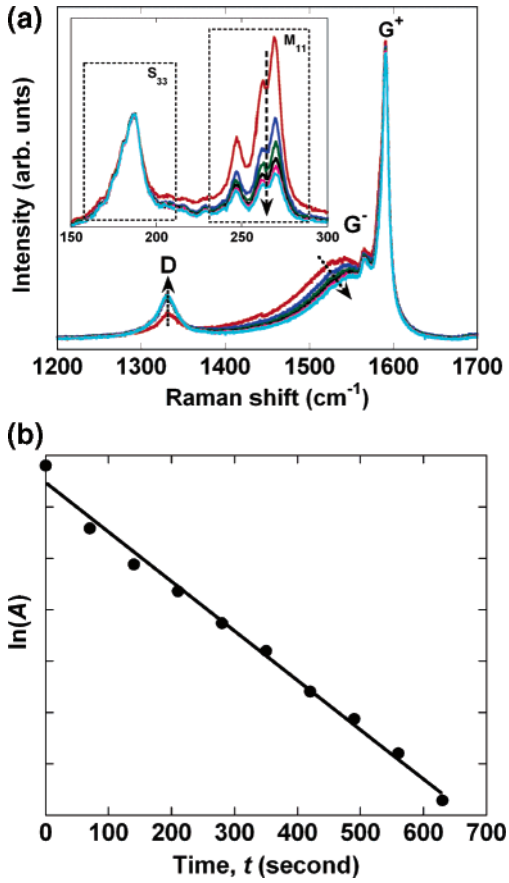

Figure 3. (a) Resonant Raman spectra at 514.5 nm wavelength for sample SED depicting the G band with the RBM section in the inset. Data were acquired sequentially each for 10 s with an interval of 60 s during laser irradiation at 20 mW. (b) Log-linear plot of the integrated intensity of the M_{11} peaks versus time of the laser irradiation (dots) with a linear fit superimposed (solid line).

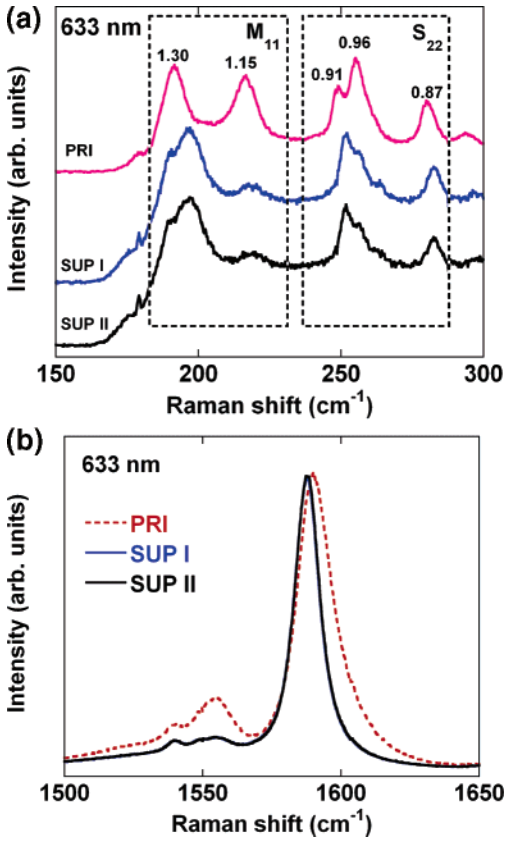

Figure 4. Resonant Raman spectra at 632.8 nm wavelength in (a) the RBM section and (b) the G band for samples PRI and SUP both acquired at 20 mW. For sample SUP, a second spectrum (II) was acquired after an interval of 2 min at the end of data acquisition for spectrum I during laser irradiation.

cm^{-1} that is attributed to m-SWNTs. For sample SUP irradiated for 4 min before data acquisition, the BWF line shape has disappeared and the remaining sharp G^+ peak at 1591 cm^{-1} and G^- peak at 1564 cm^{-1} are characteristic of s-SWNTs.[20] The BWF line shape has been shown to originate from the coupling of phonons to an electronic continuum near the Fermi energy of nanotubes.[21] The BWF line width can be decreased significantly by charge transfer as a consequence of the decrease in electron density in the continuum and therefore of the decrease in electron−phonon coupling effect in m-SWNTs.[22] Hence, the nearly complete disappearance of the BWF line shape for sample SUP in Figure 2b is likely to be caused by the formation of a charge-transfer complex through chemical bonding on the sidewall of m-SWNTs through which electrons are extracted from the continuum of the nanotubes under appropriate laser irradiation.

That Triton X-100 in combination with appropriate laser irradiation causes selective chemical interaction with m-SWNTs below 1.1 nm in diameter is better illustrated using sample SED with a much higher density of SWNTs than in sample SUP. Moreover, the majority of the SWNTs are large diameter bundles in sample SED. A time-dependent spectral decay, characteristic of chemical interaction, of the M_{11} peaks excited at 514.5 nm is evident for sample SED, see the inset in Figure 3a. The Raman spectra were sequentially recorded with a constant data acquisition time of 10 s and an interval of 60 s between two adjacent spectra, during which the laser kept irradiating the same spot at 20 mW. In the RBM section (inset in Figure 3a), the M_{11} peaks originating from m-SWNTs below 1.1 nm in diameter are successively and rapidly decreasing approaching a stable intensity. In contrast, the intensity of the S_{33} peak from s-SWNTs above 1.1 nm in diameter stays unchanged. The final stable peak intensity for the M_{11} peaks represents the contribution of m-SWNTs deep inside the bundles that are not easily accessible by Triton X-100. The integrated intensity of the M_{11} peaks, A, shows an exponential decay with time of the laser irradiation, t, as depicted in Figure 3b where the natural logarithm of A is plotted versus t. This exponential relation reflects the photon-induced surface interaction of Triton X-100 with the sidewall of m-SWNTs. Concomitantly, the BWF line shape attributed to m-SWNTs is also successively decreasing in the G band (Figure 3a). Furthermore, the disorder-induced D band at 1332 cm^{-1} experiences a rapid increase followed by saturation at a level about twice the initial peak intensity. An increase in D band indicates a conversion of sp^2 to sp^3 hybrid on m-SWNTs. Similar observation of an increase in D band has previously been found due to covalent functionalization of diazonium reagents on the sidewall of nanotubes.[16] The D band involves the resonantly enhanced scattering of an electron through phonon emission by a defect on the nanotube,[20] which

(20) Dresselhaus, M. S.; Dresselhaus, G.; Saito, R.; Jorio, A. *Phys. Rep.* **2005**, *409*, 47.
(21) Brown, S. D. M.; Jorio, A.; Corio, P.; Dresselhaus, M. S.; Dresselhaus, G.; Saito, R.; Kneipp, K. *Phys. Rev. B.* **2001**, *63*, 155414.
(22) Corio, P.; Santos, P. S.; Brar, V. W.; Samsonidze, G. G.; Chou, S. G.; Dresselhaus, M. S. *Chem. Phys. Lett.* **2003**, *370*, 675.

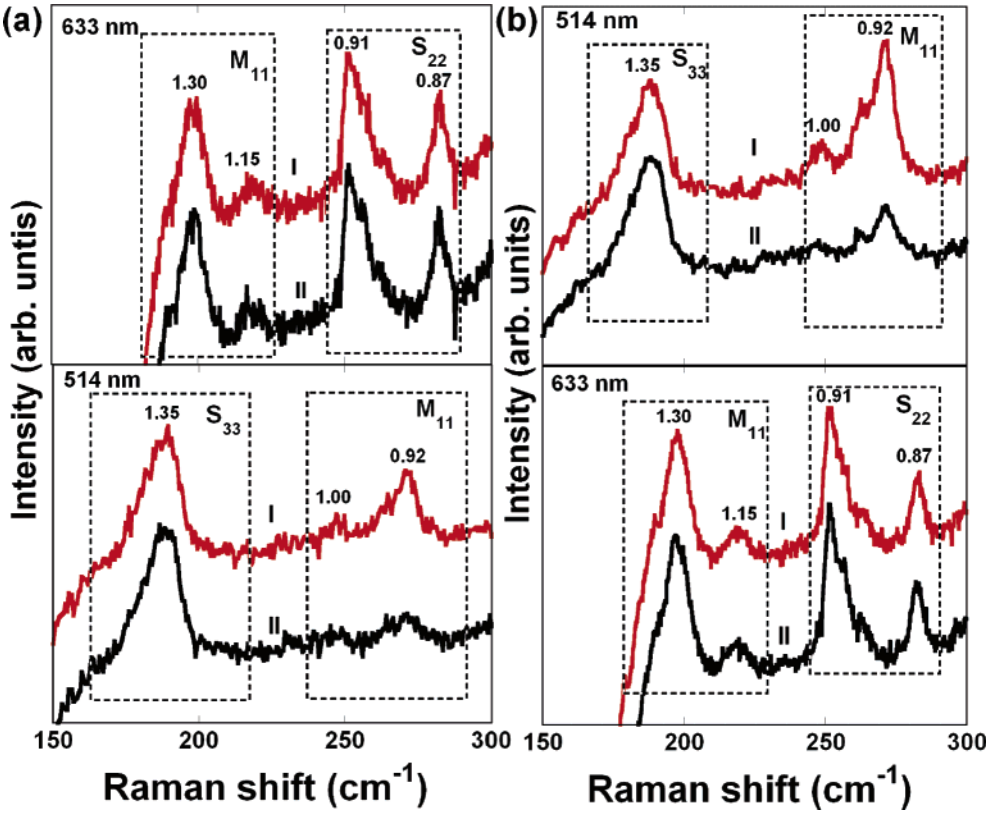

Figure 5. RBM section of Resonant Raman spectra for sample SUP, obtained (a) by first irradiation at 632.8 nm (upper panel) followed by irradiation at 514.5 nm (lower panel) on one spot, and (b) vice versa first irradiation at 514.5 nm (upper panel) followed by irradiation at 632.8 nm (lower panel) on another spot. For each case, the data were acquired twice under otherwise identical conditions, with an interval of 60 s yielding spectra I and II.

has not been observed to increase by physisorption of surfactants on nanotubes.[23] It should be noted that all the observations described so far were reproducible with the use of supernatant and sediment suspensions kept in test tubes for several weeks.

(b) Excitation at 632.8 nm. The photon energy for laser irradiation during Raman investigation is a further critical parameter for the selective interaction between SWNTs and Triton X-100, which is the focus below with an excitation at 632.8 nm. Complementary to the excitation at 514.5 nm, the excitation at 632.8 nm is simultaneously resonant with the v1 → c1 transition (M_{11}) in m-SWNTs above 1.1 nm in diameter and the v2 → c2 transition (S_{22}) in s-SWNTs below 1.1 nm in diameter. The RBM section of the Raman spectra for samples PRI and SUP is shown in Figure 4a, whereas the G band for the same samples is given in Figure 4b. In the RBM section, the M_{11} peaks at 191 and 216 cm^{-1} are assigned to m-SWNTs and the S_{22} peaks at 249, 255, and 280 cm^{-1} to s-SWNTs. The spectral upshift and the redistribution in intensity of the RBM peaks for sample SUP relative to sample PRI are again likely to be caused by physisorption of Triton X-100 on SWNTs.[19] For sample SUP, two spectra were acquired for comparison. No observable difference is found between the initial spectrum marked **I** and the second spectrum marked **II** that was obtained with an additional laser irradiation at 632.8 nm for 2 min after spectrum **I** was taken. Furthermore, the G band is identical for spectra **I** and **II** as seen in Figure 4b. These results show that the laser irradiation at 632.8 nm has made little change to either large-diameter m-SWNTs or small-diameter s-SWNTs, indicating that Triton X-100 remains physically adsorbed to the nanotubes.

Compared to the G band of sample PRI, the G^+ peak is downshifted by 2 cm^{-1} and becomes narrower and the intensity of G^- peak is decreased substantially for sample SUP. Such changes with the G band have previously been observed for a SWNT stacked with pyrene that is a planar π-conjugated surfactant.[24] Since the hydrophobic group of a Triton X-100 molecule contains a π-conjugated phenyl ring, the changes with the G band of sample SUP relative to that of sample PRI observed in Figure 4b led us to suggest that Triton X-100 molecules are absorbed by stacking their phenyl rings on the surface of the SWNTs. However, it remains unproven if the ring stacking is responsible for the subsequent chemical interaction between Triton X-100 and the SWNTs. Although less significant and slower in bleaching the Raman signals from the m-SWNTs below 1.1 nm in diameter, the use of Brij 35 that contains no phenyl ring did, indeed, lead to a reduction of the amplitude of the signals upon laser irradiation at 514.5 nm (see Supporting Information). Similar effects were also found with the use of Triton X-405, with respect to a decreased effectiveness as compared to the use of Triton X-100 in reduction of the Raman signals from the m-SWNTs below 1.1 nm in diameter upon laser irradiation at 514.5 nm (see Supporting Information). As shown in Figure 1, the only difference between Triton X-405 and Triton X-100 is a larger PEO group with the former molecule. Thus, all three surfactants

(23) Strano, M. S.; Moore, V. C; Miller, M. K; Allen, M. J; Haroz, E. H.; Kittrell, C.; Hauge, R. H; Smalley, R. E. *J. Nanosci. Nanotechnol.* **2003**, *3*, 81.

(24) Stepanian, S. G.; Karachevtsev, V. A.; Glamazda, A. Y.; Dettlaff-Weglikowska, U.; Adamowicz, L. *Mol. Phys.* **2003**, *101*, 2609.

share one thing in common (cf. Figure 1): the PEO group, but of different length. The possible role of the PEO group and its length in the reaction to SWNTs needs to be clarified; such an elaborated investigation is however beyond the scope of the present work.

Finally, in order to shed more light on the effect of laser wavelength on the M_{11} peaks for small-diameter m-SWNTs as seen in Figures 2 and 3, a combined laser irradiation was arranged for sample SUP. Two sequential irradiations were made: (1) irradiation first at 632.8 nm (upper panel in Figure 5a) followed by irradiation at 514.5 nm (lower panel in Figure 5a) on one spot, and (2) vice versa with irradiation first at 514.5 nm (upper panel in Figure 5b) followed by irradiation at 632.8 nm (lower panel in Figure 5b) on another spot. All irradiations were performed at 20 mW during which continuous data acquisition for 30 s was carried out twice with an interval for 60 s between the two data acquisitions, resulting in two Raman spectra (spectra **I** and **II**) for each case. In the upper panel of Figure 5a, no difference between spectra **I** and **II** is resulted by the irradiation at 632.8 nm concerning the M_{11} peaks originating from m-SWNTs above 1.1 nm in diameter, in agreement with the results in Figure 4a. Once again, no change is seen with the S_{22} peaks, as expected. In the lower panel of Figure 5a, a substantial decrease of the M_{11} peaks originating from m-SWNTs below 1.1 nm in diameter is clearly observable with the irradiation at 514.5 nm. The decrease of the M_{11} peaks is obviously independent of the prior irradiation at 632.8 nm. In the upper panel of Figure 5b, a substantial decrease of the M_{11} peaks originating from m-SWNTs below 1.1 nm in diameter is immediately found by the irradiation at 514.5 nm. However, the irradiation at 514.5 nm apparently has no influence on the m-SWNTs above 1.1 nm in diameter, since the M_{11} peaks excited at 632.8 nm remain unaltered between spectra **I** and **II** in the lower panel of Figure 5b. Therefore, the decrease of the M_{11} peaks for the small-diameter m-SWNTs was induced only by photons with energies coinciding with the electronic transitions in these m-SWNTs. Irradiation with photons whose energies deviated from the electronic transitions did not lead to any spectral decay.

(c) Energetics. With the experimental results at hand, we are unable to identify the precise nature of the chemical interaction being examined, e.g., covalent, redox, etc. Clearly, more work is required for this purpose. From the energetic point of view, the initial physisorption of Triton X-100 on the SWNTs indicates that the energy level at which the chemical interaction takes place is above the Fermi level of the nanotubes. Laser irradiation causes excitation of electrons in the SWNTs from the energy states below the Fermi level to the energy states above. The excellent selectivity preferring m-SWNTs with respect to bleaching their Raman signals indicates the paramount importance of the density of electrons near the Fermi level in the continuum between the first pair of van Hove singularities of the m-SWNTs. Provided with the excited electrons of the required energy for the chemical interaction, a charge-transfer complex with chemical bonds that first form on the sidewall of m-SWNTs facilitates transfer of the excited electrons, which gives rise to a decrease in the BWF line width and an increase in the intensity of the D band for the m-SWNTs as shown in Figure 3a. Since there is no energy state between the first pair of van Hove singularities of s-SWNTs, such a charge-transfer complex cannot form. Hence, the physisorption of Triton X-100 on s-SWNTs prevails even with laser irradiation. Furthermore, the distinct selectivity preferring the small-diameter m-SWNTs in Figure 5 points to the important role of curvature-induced strain energy in the conversion from physisorptions to chemical interaction between Triton X-100 and m-SWNTs. The curvature-induced strain energy in a nanotube per carbon atom, including contributions of pyramidalization and π-orbital misalignment, has been shown to be inversely related to nanotube diameter.[25,26] It has been predicted that nanotubes of smaller diameter are more susceptible to chemical reagent,[27] which has been shown to be responsible for the diameter dependence of chemical reaction between nanotubes and various chemical reagents.[2,5] The process for the interaction between Triton X-100 and SWNTs under laser irradiation can hence be briefly described as follows. Initially, Triton X-100 molecules are physically adsorbed on SWNTs, irrespective of the type and diameter of the SWNTs in condensed aqueous solution. Under laser irradiation with an appropriate excitation energy, the bonding between Triton X-100 and small-diameter m-SWNTs is converted to chemical in nature, while the physisorption of Triton X-100 on s-SWNTs of all diameters and large-diameter m-SWNTs remain unaltered.

Conclusions

The results shown in this work clearly demonstrate a photon-induced decay of Raman signals for m-SWNTs below 1.1 nm in diameter dispersed in condensed aqueous Triton X-100. Such a decay is absent for s-SWNTs of all diameters investigated as well as for m-SWNTs above 1.1 nm in diameter. The energy of the irradiating photons plays a vital role; photons of 514.5 nm wavelength are effective while those of 632.8 nm wavelength cause no effect. Since physisorption of Triton X-100 on nanotubes before laser irradiation is evident for all SWNTs irrespective of type and diameter, and since chemical bonding leads to a spectral decay, laser irradiation is concluded to provide a necessary, but not sufficient, means for a conversion from physical to chemical bonding of Triton X-100 on the sidewall of SWNTs. The mechanism of how the laser irradiation induces the conversion and the nature of the chemical interaction between m-SWNTs and Triton X-100 are unclear at present and remain to be confirmed. Our findings in the present work can nonetheless be of practical implications for selective separation and functionalization of SWNTs for nanotube-based sensors and electronic devices.

Acknowledgment. The authors would like to thank Mattias Hammar for access to the Raman measurement setup. This work was supported by the Swedish Research Council (VR) (Dnr. 621-2005-5971) and the Swedish Agency for Innovation Systems (VINNOVA) (Dnr. 2005-01138).

Supporting Information Available: Resonant Raman spectra in the RBM section are provided for raw HiPCO SWNTs dispersed in aqueous sodium dodecylbenzene sulfonate (SDBS) solution (Figure S1) as well as in aqueous Triton X-100 (Figure S2), Triton X-405 (Figure S3), and Brij 35 (Figure S4) solutions.

JA066419S

(25) Haddon, R. C. *Acc. Chem. Res.* **1988**, *21*, 243.
(26) Chen, Z.; Thiel, W.; Hirsch, A. *Chem. Phys. Chem.* **2003**, *4*, 93.
(27) Niyogi, S.; Hamon, A.; Hu, H.; Zhao, B.; Bhowmik, P.; Sen, R.; Itkis, M. E.; Haddon, R. C. *Acc. Chem. Res.* **2002**, *35*, 1105.